PHYSICAL REVIEW B **83**, 100404(R) (2011)

Valence-bond crystal in the extended kagome spin-$\frac{1}{2}$ quantum Heisenberg antiferromagnet: A variational Monte Carlo approach

Yasir Iqbal,[1] Federico Becca,[2] and Didier Poilblanc[1]

[1]*Laboratoire de Physique Théorique UMR-5152, CNRS and Université de Toulouse, F-31062, France*

[2]*Democritos National Simulation Center, Istituto Officina dei Materiali del CNR and Scuola Internazionale Superiore di Studi Avanzati (SISSA), Via Bonomea 265, I-34136 Trieste, Italy*

(Received 19 November 2010; published 7 March 2011)

The highly frustrated spin-$\frac{1}{2}$ quantum Heisenberg model with both nearest (J_1) and next-nearest (J_2) neighbor exchange interactions is revisited by using an extended variational space of projected wave functions that are optimized with state-of-the-art methods. Competition between modulated valence-bond crystals (VBCs) proposed in the literature and the Dirac spin liquid (DSL) is investigated. We find that the addition of a *small* ferromagnetic next-nearest-neighbor exchange coupling $|J_2| > 0.09J_1$ leads to stabilization of a 36-site unit cell VBC, although the DSL remains a local minimum of the variational parameter landscape. This implies that the VBC is not trivially connected to the DSL; instead it possesses a nontrivial flux pattern and large dimerization.

DOI: 10.1103/PhysRevB.83.100404 PACS number(s): 75.10.Kt, 75.10.Jm, 75.40.Mg

Introduction. It is well known that, on the nonbipartite two-dimensional Kagomé lattice, the combination of low spin ($S = 1/2$), low coordination number ($z = 4$), and frustrating antiferromagnetic (AF) exchange interactions lead to extremely strong quantum fluctuations. It is, however, a widely debated and long-standing theoretical issue whether the ground state of the nearest-neighbor (n.n.) spin-1/2 quantum Heisenberg antiferromagnet (QHAF) on the Kagomé lattice is a spin disordered state (quantum spin liquid),[1,2] which preserves spin rotation and lattice space group symmetry, or instead a valence bond crystal (VBC),[3–7] which breaks lattice symmetries. On the experimental side, studies on a nearly perfect spin-1/2 Kagomé compound, Herbertsmithite $ZnCu_3(OH)_6Cl_2$,[8–15] reveal the absence of any spin ordering down to 50 mK despite a sizable n.n. AF exchange coupling ($J \approx 180$ K) between spin-1/2 moments of Cu^{2+}. In particular, Raman spectroscopic data on Herbertsmithite points towards a gapless, algebraic spin liquid state.[16] This lends support to the view that the ground state of the n.n. spin-1/2 QHAF model on the Kagomé lattice is a long-range resonating-valence bond state. Within a class of variational projected wave functions, a particular gapless spin liquid belonging to the class of algebraic spin liquids, the U(1) Dirac state, has been claimed to possess the lowest energy.[17,18] In such a state, the (mean-field) Fermi surface collapses to two points, where the spectrum becomes relativistic with Dirac conical excitations. On the contrary, a recent study of the n.n. spin-1/2 QHAF model using density-matrix renormalization group (DMRG),[19] establishes the ground state to be a singlet-gapped spin liquid, supposedly with a Z_2 low-energy gauge structure.

From the experimental point of view, the weak ferromagnetism observed in Herbertsmithite has been attributed to the ferromagnetic (FM) nature of the next-nearest-neighbor (n.n.n.) coupling between Cu^{2+} ions in the Kagomé layers. This model was investigated in Ref. 20 by using projected wave functions and it has been found that, above a certain critical n.n.n. FM coupling, a gapless spin liquid with a large circular spinon Fermi surface, named here as uniform projected Fermi sea (PFS), is stabilized as opposed to the $U(1)$ Dirac state. Furthermore, this state undergoes a small dimerization, which lowers slightly its energy. The same n.n.n. FM model was also recently investigated using a quantum dimer model approach in Ref. 21, showing consistently that a 36-site cell VBC order is favored.

In this Rapid Communication, we revisit the spin-1/2 QHAF with the inclusion of n.n.n. exchange interactions using a more extended variational space of projected wave functions that may be optimized by using the technique of Ref. 22. In the following, we will limit to nonmagnetic variational states and, therefore, we will not consider possible instabilities toward magnetically ordered states.[23] Our main result is that the addition of ferromagnetic n.n.n. exchange coupling leads to the stabilization of a 36-site unit cell VBC (in agreement with the results of Ref. 21) over an extended ferromagnetic region which starts from a very weak coupling. Although being a dimerization of the uniform PFS, our VBC does not arise from a local instability of the latter. In other words, it is not trivially connected to it in the variational parameter landscape; instead it possesses a nontrivial flux pattern and dimerization. Moreover, we find that the level crossing between the PFS and the $U(1)$ Dirac state (once suitably extended with n.n.n. hopping) occurs at nearly twice the value previously reported.[20] For AF n.n.n. exchange coupling, the inclusion of n.n.n. hoppings in the $U(1)$ Dirac state leads to a considerable lowering in energy, which becomes more pronounced with increasing the AF coupling. Moreover, no VBC order is found in the AF n.n.n. coupling region.

Model and wave function. The Hamiltonian for spin-1/2 quantum Heisenberg J_1-J_2 model is

$$\hat{\mathcal{H}} = J_1 \sum_{\langle ij \rangle} \hat{\mathbf{S}}_i \cdot \hat{\mathbf{S}}_j + J_2 \sum_{\langle\langle ij \rangle\rangle} \hat{\mathbf{S}}_i \cdot \hat{\mathbf{S}}_j, \qquad (1)$$

where $\langle ij \rangle$ and $\langle\langle ij \rangle\rangle$ denote sums over n.n. and n.n.n. neighbor sites, respectively. In the following, we will consider $J_1 > 0$ and both FM and AF superexchange J_2; all energies will be given in units of J_1.

The variational wave functions are defined by projecting noncorrelated fermionic states:

$$|\Psi_{\mathrm{VMC}}(\chi_{ij}, \Delta_{ij}, \mu)\rangle = \mathcal{P}_G |\Psi_{\mathrm{MF}}(\chi_{ij}, \Delta_{ij}, \mu)\rangle, \qquad (2)$$

where $\mathcal{P}_G = \prod_i (1 - n_{i,\uparrow} n_{i,\downarrow})$ is the full Gutzwiller projector enforcing the one fermion per site constraint. Here, $|\Psi_{\rm MF}(\chi_{ij}, \Delta_{ij}, \mu)\rangle$ is the ground state of mean-field Hamiltonian containing chemical potential, hopping, and pairing terms:

$$\mathcal{H}_{\rm MF} = \sum_{i,j,\alpha} (-\chi_{ij} + \mu \delta_{ij})\, c^\dagger_{i,\alpha} c_{j,\alpha} + \Delta_{ij} c^\dagger_{i,\alpha} c^\dagger_{j,-\alpha} + \text{h.c.} \qquad (3)$$

In this work, all states that we consider include hopping terms only (i.e., χ_{ij} up to second neighbors). The effect of including BCS pairing terms is discussed at the end of this Rapid Communication. Cases in which the translational symmetry is explicitly broken will also be considered, so as to include VBC states.

Different spin liquid and VBC phases correspond to different patterns of distribution of χ_{ij} and Δ_{ij} on the lattice bonds; they are the *ansatz* of a given state and serve as the variational parameters that are optimized within the variational Monte Carlo scheme to find the energetically best state.[22] It is worth mentioning that this method allows us to obtain an extremely accurate determination of variational parameters. All parameters belonging to one class (i.e., with the same magnitude) are generically labeled as χ_λ.

Results. We have performed our variational calculations on a 576-site (i.e., $36 \times 4 \times 4$) cluster with mixed periodic-antiperiodic boundary conditions. Such a cluster accommodates all possible VBC supercells proposed in the literature. In addition, it ensures nondegenerate wave functions at half-filling.

For n.n. spin-1/2 QHAF, among the class of n.n. translationally symmetric, nonchiral, gapless spin liquids, the $U(1)$ Dirac state is given by the *ansatz* in Fig. 1(a). Due to flux φ being 0 and π [$\exp(i\varphi) = \prod_{\rm plaquette} \chi_\lambda$] through the triangles and hexagons, respectively, it is denoted as $[0,\pi]$. Its energy per site is $E/J_1 = -0.42866(1)$. The n.n. uniform PFS state has no flux through any plaquette and is therefore denoted as [0,0]; its energy per site is $E/J_1 = -0.41197(1)$.[17,18] In this work we study only gapless states in particular those with a $U(1)$ low energy gauge structure. However, we believe that by performing a case by case projected wave function study of all possible (a few hundred) Z_2 spin liquids on the Kagomé lattice, one can identify variationally the state found in Ref. 19 using DMRG.

With the aim of investigating the effect of an additional n.n.n. exchange coupling (of both AF and FM type), we first extend the $[0,\pi]$ and [0,0] states. While previous studies,[20] considered wave functions with n.n. couplings only, here we include in addition n.n.n. couplings in the mean-field Hamiltonian (3), which also leads to space group symmetric, nonchiral, gapless spin liquids (see Fig. 1). Two new plaquettes (triangles *abc* and *acd* in Fig. 1) appear upon the inclusion of n.n.n. couplings. Space group symmetric, nonchiral spin liquids may now be labeled by four fluxes (but only three are independent) (i.e., by $[\alpha,\beta;\gamma,\delta]$, α and β are fluxes through original triangles and hexagons, respectively; γ and δ instead are fluxes through triangles *abc* and *acd*, respectively). The only possible states built upon the $[0,\pi]$ state are $[0,\pi;\pi,0]$ or $[0,\pi;0,\pi]$ and those upon the [0,0] state are $[0,0;\pi,\pi]$ or [0,0;0,0] (see Fig. 1). Notice that for both DSL and PFS, the two states with different γ and δ fluxes are related by a change of sign in $\chi_{\rm n.n.n.}$. The energetically lower states will depend upon the actual value of the ratio J_2/J_1. This extension does not modify the topological properties associated with the wave functions, such as the Dirac spectrum and the large spinon Fermi surface. Most importantly, the inclusion of n.n.n. hopping parameters leads to lowering of the variational energies, via an optimal tuning of $\chi_{\rm n.n.n.}$ as a function of J_2 [see Fig. 2(a)]. It is important to note that we purposely restrict our calculations to small enough J_2/J_1, since for larger n.n.n. couplings (of both AF and FM type), it is probable that Néel states are energetically favored, and consequently our treatment becomes insufficient.

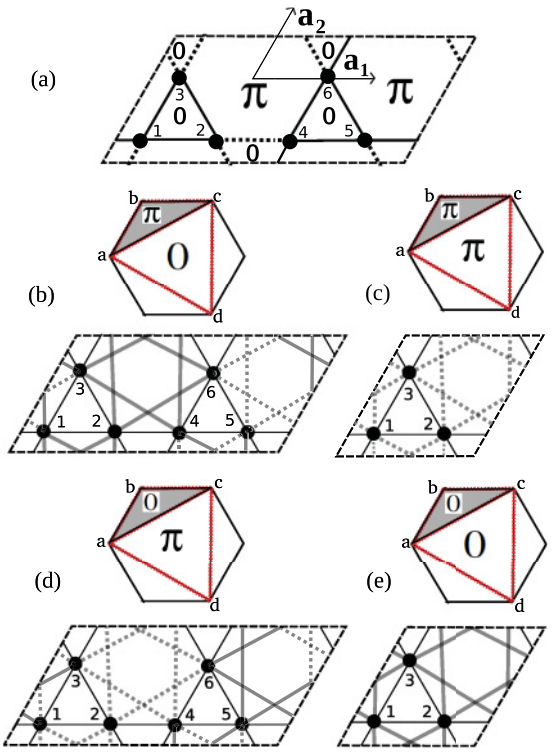

FIG. 1. (Color online) The $U(1)$ DSL *ansatz*, solid (dashed) bonds denote positive (negative) hoppings (a). The unit cell is doubled to accommodate $[0,\pi]$ flux. Cases with n.n.n. hopping are also reported; the only possible (nonchiral) space group symmetric states built upon $[0,\pi]$ state are $[0,\pi;\pi,0]$ (b) or $[0,\pi;0,\pi]$ (d) and those upon the uniform [0,0] state (i.e., PFS) are $[0,0;\pi,\pi]$ (c) or [0,0;0,0] (e).

Point D in Figs. 2(b) and 3 marks a transition between the [0,0;0,0] and $[0,0;\pi,\pi]$ states, and point E the transition between $[0,\pi;0,\pi]$ and $[0,\pi;\pi,0]$ states, both occurring at $J_2 \neq 0$. Therefore, we find a finite $\chi_{\rm n.n.n.}$ even for the n.n. spin-1/2 QHAF [see points F and G in Fig. 2(b)]. We mention that these extended wave functions with n.n.n. hoppings lead to slightly lower energies, namely $E/J_1 = -0.42872(1)$ for the $[0,\pi;0,\pi]$ state and $E/J_1 = -0.41209(1)$ for the $[0,0;\pi,\pi]$ state.

Due to negative n.n.n. spin-spin correlations of $[0,\pi]$ state and positive for the [0,0] state, a level crossing occurs at $J_2/J_1 \approx -0.16$[20] (see point B in Fig. 3). However, the addition of the n.n.n. hopping shifts the level crossing between the reference spin liquids, the [0,0;0,0] and $[0,\pi;0,\pi]$ states to $J_2/J_1 \approx -0.335$ (see point A in Fig. 3).

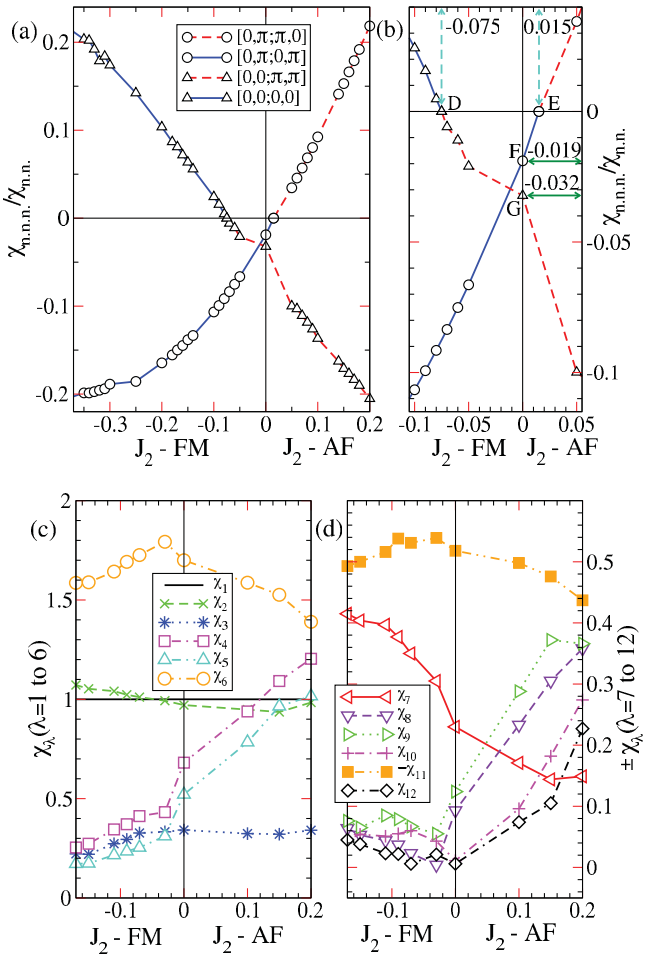

FIG. 2. (Color online) (a) Optimized $\chi_{\text{n.n.n.}}/\chi_{\text{n.n.}}$ versus J_2 for the extended PFS and DSL states of Fig. 1. A zoom around $J_2 = 0$ is shown in (b). The optimized n.n. (c) and n.n.n. (d) hopping parameters versus J_2 for the 36-site supercell VBC are also reported. $\chi_1 = 1$ is the reference bond. Only $\chi_{11} < 0$, which implies $[0,0;\pi,\pi]$ flux in the P hexagons of Fig. 4.

The question of global and local instability of these spin-liquid states toward a VBC ordering is now thoroughly addressed. In contrast to previous studies,[17,20] which aimed at checking only the local instabilities of spin liquids toward various dimerization patterns via the imposition of a small bond amplitude modulation (5%–10%) of χ_λ, we make a complete optimization of the parameters to detect a possible stabilization of VBC states.

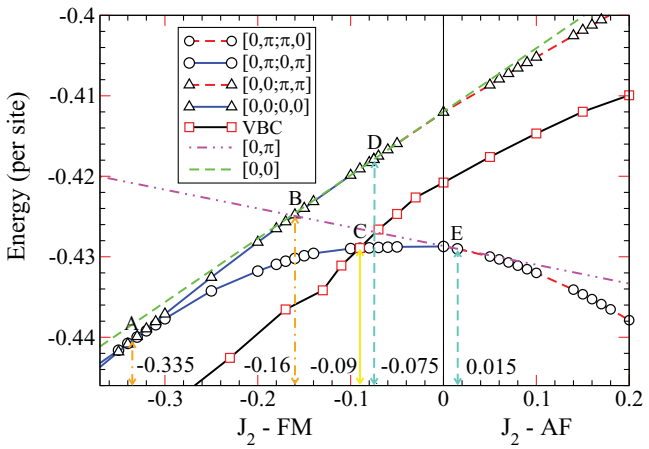

FIG. 3. (Color online) Energy versus J_2 for spin liquid (see Fig. 1) and VBC states [see Figs. 4(c) and 4(d)].

In the 12-site supercell, all bonds connected by D_6 operations have the same magnitude [see Fig. 4(a)], leading to three classes of different bonds. In the 18-site supercell [see Fig. 4(b)], there are only two classes of bonds. In the 36-site supercell with n.n. couplings [see Fig. 4(c)], there are six classes, given the D_6 symmetry about the hexagon C. By adding n.n.n. bonds and preserving this symmetry, we obtain six more independent bonds [see Fig. 4(d)].

In our analysis, we start from a large number of arbitrary different points (amplitude modulation of χ_λ) in the variational space and thoroughly scan the landscape. As a consequence we find that for the n.n. spin-1/2 QHAF, the $[0,\pi]$ and [0,0] states are locally and globally stable with respect to 12-site,[4] 18-site,[3,20] and 36-site[3,5–7] supercell dimerizations. Indeed, the optimization procedure always gives back the uniform $|\chi_\lambda| = 1$ state. We bring attention to the fact that the 36-site supercell considered by us has a much larger variational space

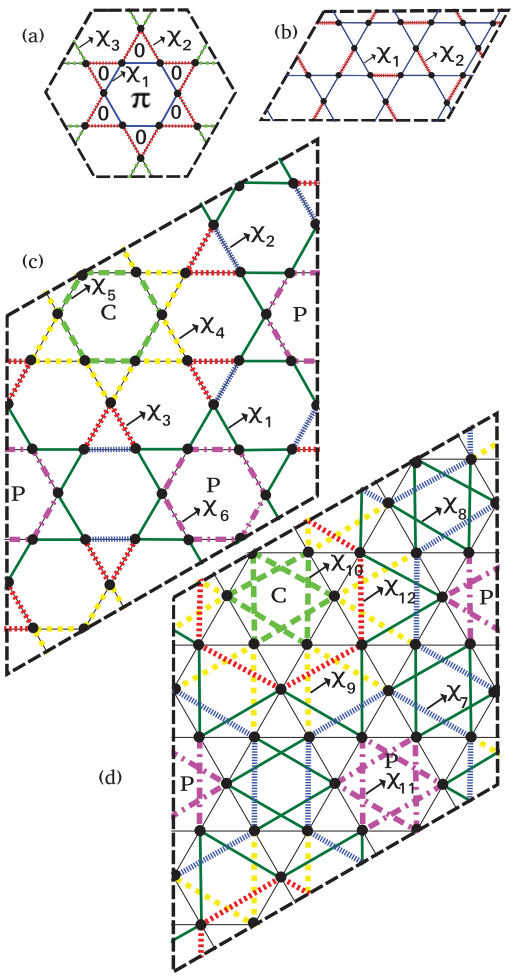

FIG. 4. (Color online) Twelve-site supercell (a) with three different parameters for the hopping; 18-site supercell with two different parameters; 36-site supercell with six n.n. parameters (c), and with six n.n.n. parameters (d).

(six different hoppings) as compared to the ones studied in literature, which considered a dimerization only along the hexagon P in Fig. 4(c).

Upon the inclusion of a finite FM J_2, we detect the appearance of another competing state with broken symmetries which is stabilized and is the lowest in energy for $J_2 < -0.09$ (see point C in Fig. 3). This state is found to be a 36-site supercell VBC, shown in Figs. 4(c) and 4(d). It breaks translational symmetry in the magnitude of the n.n. and n.n.n. order parameters and the $[\gamma,\delta]$ fluxes but preserves the rotation and reflection symmetry in both magnitude of χ_λ and $[\alpha,\beta;\gamma,\delta]$ fluxes. The corresponding state has 12 different hopping parameters. Although we obtain this VBC as a dimerization of the [0,0; 0,0] state, it is not a local instability of it. Instead, it possesses a large bond amplitude modulation in the extended variational space of n.n. and n.n.n. order parameters and selects a flux pattern with $[\gamma,\delta]$ fluxes being $[\pi,\pi]$ in the P hexagons which form a honeycomb lattice [see Fig. 4(d)]. On the contrary, all other hexagons have [0,0] fluxes. The optimized χ_λ as a function of J_2 are shown in Figs. 2(c) and 2(d). In a previous work, which investigated the effect of a J_2 FM exchange coupling using projected variational wave functions,[20] it was found that a dimer modulation leads to an energy minimum at $J_2/J_1 \approx -0.16$, for approximately 4% bond amplitude modulation. In contrast, we find a different VBC wave function, which is stabilized starting from a very weak FM n.n.n. coupling. As mentioned above, this state possesses a very large 36-site modulation, leading to a significant large gain in energy.

We finish by considering the case of an AF J_2 coupling. Our study reveals the absence of symmetry breaking; instead we find a gapless state with Dirac fermions, the $[0,\pi;\pi,0]$ state. Upon optimizing $\chi_{\text{n.n.n.}}/\chi_{\text{n.n.}}$, this state gets a significantly lower energy than the n.n. $[0,\pi]$ state, this gain becoming more pronounced for larger J_2 (see Fig. 3). Finally, the addition of a BCS pairing term of the s-wave type in the $[0,\pi;\pi,0]$ wave function for J_2 AF is also studied, and our calculations show that such an inclusion always increases the energy. However, the effect of including other forms of pairing terms which might stabilize a gapped spin liquid or a VBC in the J_2 AF model is left as a direction of future research. This might provide a reconciliation with the exact diagonalization results of Ref. 24, which point toward an opening of a gap upon addition of a small AF J_2 coupling.

In summary, we investigated the spin$-1/2$ QHAF on the Kagomé lattice by using improved variational wave functions. We found that a VBC is stabilized when an n.n.n. ferromagnetic superexchange coupling is considered. This state possesses a nontrivial distribution of hopping parameters and flux pattern.

[1] P. W. Anderson, Mater. Res. Bull. **8**, 153 (1973).
[2] P. W. Anderson, Science **235**, 1196 (1987).
[3] J. B. Marston and C. Zeng, J. Appl. Phys. **69**, 5962 (1991).
[4] M. B. Hastings, Phys. Rev. B **63**, 014413 (2000).
[5] P. Nikolic and T. Senthil, Phys. Rev. B **68**, 214415 (2003).
[6] R. R. P. Singh and D. A. Huse, Phys. Rev. B **76**, 180407(R) (2007).
[7] D. Poilblanc, M. Mambrini, and D. Schwandt, Phys. Rev. B **81**, 180402(R) (2010); D. Schwandt, M. Mambrini, and D. Poilblanc, *ibid.* **81**, 214413 (2010).
[8] A. Olariu, P. Mendels, F. Bert, F. Duc, J. C. Trombe, M. A. de Vries, and A. Harrison, Phys. Rev. Lett. **100**, 087202 (2008).
[9] F. Bert, S. Nakamae, F. Ladieu, D. L'Hôte, P. Bonville, F. Duc, J.-C. Trombe, and P. Mendels, Phys. Rev. B **76**, 132411 (2007).
[10] P. Mendels, F. Bert, M. A. de Vries, A. Olariu, A. Harrison, F. Duc, J. C. Trombe, J. S. Lord, A. Amato, and C. Baines, Phys. Rev. Lett. **98**, 077204 (2007).
[11] T. Imai, E. A. Nytko, B. M. Bartlett, M. P. Shores, and D. G. Nocera, Phys. Rev. Lett. **100**, 077203 (2008).
[12] O. Ofer, A. Keren, E. A. Nytko, M. P. Shores, B. M. Bartlett, D. G. Nocera, C. Baines, and A. Amato, e-print arXiv:cond-mat/0610540 (2006).
[13] J. S. Helton, K. Matan, M. P. Shores, E. A. Nytko, B. M. Bartlett, Y. Yoshida, Y. Takano, A. Suslov, Y. Qiu, J.-H. Chung, D. G. Nocera, and Y. S. Lee, Phys. Rev. Lett. **98**, 107204 (2007).
[14] S.-H. Lee, H. Kikuchi, Y. Qiu, B. Lake, Q. Huang, K. Habicht, and K. Kiefer, Nat. Mater. **6**, 853 (2007).
[15] M. A. de Vries, K. V. Kamenev, W. A. Kockelmann, J. Sanchez-Benitez, and A. Harrison, Phys. Rev. Lett. **100**, 157205 (2008).
[16] D. Wulferding, P. Lemmens, P. Scheib, J. Röder, P. Mendels, S. Chu, T. Han, and Y. S. Lee, Phys. Rev. B **82**, 144412 (2010).
[17] Y. Ran, M. Hermele, P. A. Lee, and X.-G. Wen, Phys. Rev. Lett. **98**, 117205 (2007).
[18] M. Hermele, Y. Ran, P. A. Lee, and X.-G. Wen, Phys. Rev. B **77**, 224413 (2008).
[19] S. Yan, D. A. Huse, and S. R. White, e-print arXiv:1011.6114 (2010).
[20] O. Ma and J. B. Marston, Phys. Rev. Lett. **101**, 027204 (2008).
[21] D. Poilblanc and A. Ralko, Phys. Rev. B **82**, 174424 (2010).
[22] S. Yunoki and S. Sorella, Phys. Rev. B **74**, 014408 (2006).
[23] P. Lecheminant, B. Bernu, C. Lhuillier, L. Pierre, and P. Sindzingre, Phys. Rev. B **56**, 2521 (1997).
[24] P. Sindzingre and C. Lhuillier, Euro. Phys. Lett. **88**, 27009 (2009).